

Direct Observation of Electromigration of Si Magic Clusters on Si(111) Surfaces

Mon-Shu Ho,^{1,2} Ing-Shouh Hwang,¹ and Tien T. Tsong¹

¹*Institute of Physics, Academia Sinica, Nankang, Taipei, Taiwan, Republic of China*

²*Department of Physics, Pennsylvania State University, University Park, Pennsylvania 16802*

(Received 5 November 1999)

Using scanning tunneling microscopy, we have observed electromigration of Si on Si(111)-(7 × 7) surfaces and have identified the diffusion species to be Si magic clusters. Effects of the directed motion along the direction of the heating current in electromigration and those in thermal migration are determined separately and quantitatively. We also observe the preferential filling of two-dimensional (2D) Si craters and the preferential detachment of Si magic clusters from the edges of 2D Si islands near the cathode side. The driving force for this anisotropic behavior is much stronger than previously recognized.

PACS numbers: 66.30.Qa, 36.40.Sx, 66.10.Cb

Electromigration is mass transport in a preferred direction, or biased diffusion, caused by a direct electric current in the sample. In contrast, particles undergo random walk without a preferred direction in thermally activated diffusion. Electromigration has been identified to be the major cause for failure of interconnects in integrated circuits [1–3]. As components in microelectronic devices continue to reduce in size to nanometer scale, understanding of this effect and a search of methods for preventing it will become more and more important. Moreover, electromigration is a phenomenon of fundamental interest to surface, condensed matter, and materials sciences. Recent experimental studies demonstrate that annealing with a direct current can have a profound influence on the development of surface morphology [3–7]. One of the most intriguing observations is on the Si(111) surface. It develops bunches of steps separated by wide step-free terraces when the sample is resistively heated to temperatures above 900 °C with current of a certain direction [5,7]. It was also reported that direct current heating of a copper film results in formation of voids at the cathode side and hillocks at the anode side [3]. Surface electromigration is believed to be responsible for all these observations. In spite of great efforts over the last several decades, the nature of the driving force of this effect remains unclear [8]. A major reason is the lack of direct observation of individual diffusion events and species.

In this Letter, we find that a special type of Si magic cluster exhibits directed long jumps along the direction of the heating current on Si(111)-(7 × 7) surfaces. Effects of electromigration and the thermal migration are determined separately and quantitatively. We also observe the preferential presence of Si magic clusters at the corner of Si craters near the cathode side and their subsequent attachment to that corner as well as the preferential detachment of Si magic clusters from Si bilayer island edges near the cathode side. As the electric fields we apply are very small, the strong tendency for these biased phenomena is very surprising. These observations may provide important clues for microscopic understanding of the driving force of

electromigration and the morphology change caused by direct current heating.

Our experiments are performed using a JOEL scanning tunneling microscope (STM) (JSTM-4500VT) in an ultrahigh vacuum chamber with a base pressure of 5×10^{-11} torr. The preparation of a clean Si(111)-(7 × 7) surface and the operation of continuous-time STM imaging at elevated temperatures have been described previously [9]. With the STM, we have recently found a special type of Si magic cluster on clean Si(111) surfaces [10]. They are the fundamental units of mass transport, step fluctuations, and epitaxial growth on this surface. Figures 1(a) and 1(b) show a filled-state and an empty-state image of a Si magic cluster, respectively. These clusters are mobile at temperatures above ~ 400 °C. Most of the time, the cluster hops within a half cell of Si(111)-(7 × 7), but sometimes it hops out of its original half [10]. Using continuous-time scanning, we have measured the rates of hopping within and out of a half cell from which the activation energies are determined to be ~ 2 eV [10]. These energies are close to one Si-Si bond strength of the bulk. Presumably, Si atoms in the clusters are so tightly bound that their interaction with the substrate is greatly weakened.

Interestingly, when a Si magic cluster hops out of a half cell, it usually reappears at a site a few hundred Å away. Hops to a neighboring half cell are rarely seen. An

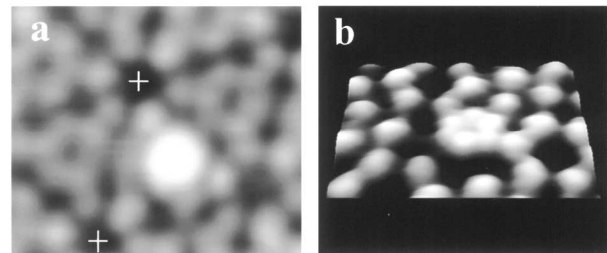


FIG. 1. (a) STM images of a Si magic cluster taken at the sample bias of -1.5 V. The spacing between two neighboring corner holes (indicated by “+”) is 27 Å. (b) 3D view of the magic cluster taken at the sample bias of $+1.2$ V.

example of long hops is shown in Fig. 2. A defect O , which is immobile throughout our observation (~ 2 h), serves as a marker. A Si magic cluster at the upper left-hand corner [indicated with a white arrow in Fig. 2(a)] disappears at $t = 120$ s [Fig. 2(b)], but one is seen immediately at the lower side of the image. Since the hopping rate and the concentration of Si magic clusters are ~ 0.002 s $^{-1}$ and $\sim 2 \times 10^{-7}$ Å $^{-2}$, respectively, at 450 °C, we conclude that they are the same cluster [11]. Later, another Si cluster appears at a site near the defect O [Fig. 2(c)]. This new cluster (indicated by a black arrow) hops downward sometime later [Fig. 2(d)]. Another 10 s later, this cluster hops to the lower left-hand side [Fig. 2(e)]. Since we do not see any trace of the Si clusters at intermediate positions, they should have a much lower diffusion barrier (< 1.5 eV) during the long jumps. Probably, only Si clusters at stable adsorption sites can have a lifetime long enough to be imaged by the STM. These clusters may be bonded to certain 7×7 sites at a certain orientation. The long jumps may arise from frustration for the magic cluster to connect properly with substrate chemical bonds once they are broken. This mechanism is analogous to the slip diffusion proposed by Luedtke and Landman [12] in their molecular dynamics simulations of a Au $_{140}$ cluster on graphite. Recently, Krylov also predicted that long jumps could occur for large clusters with strong intracluster interactions and weak cluster-substrate interactions [13]. A detailed theoretical study of our system will gain insight to understanding the mechanism of long jumps of large clusters.

The most interesting behavior seen in the long hops of Si magic clusters is that the clusters have a bias (65%–80%) for motion in the direction toward the cathode, as shown in Fig. 2. To separate electromigration from thermal migration, we resolve all the displacements of long hops

into components parallel to the current, x components, and components perpendicular to the current, y components. The latter arises from thermal migration, and the former includes the effect of electromigration. The algebraic average of all the x components, D_{EM} , represents the average net displacement due to electromigration. The net displacement due to thermal migration vanishes, since thermal migration is equally probable in $+x$ and $-x$ directions. For the mere purpose of comparing D_{EM} with thermal migration length, L_{TH} , we calculate the root mean square of all the y components and multiply it by $\sqrt{2}$ to account for two-dimensional diffusion. The temperature dependences of both D_{EM} and L_{TH} are shown in Fig. 3. If there were no electromigration, D_{EM} should vanish. The fact that they are nonzero confirms most directly and quantitatively the occurrence of electromigration of individual clusters.

We also create 2D craters (one bilayer deep) by applying an electric pulse to the STM tip at elevated temperatures [14,15]. Our subsequent STM images show the presence of magic clusters inside the craters and their subsequent incorporation into the crater edge. Figures 4(a)–4(d) are four images chosen from our continuous-time scan of intervals 9.2 s each. Figure 4(a) shows the preferential presence of magic clusters at the lower left-hand corner of the crater. Figures 4(b)–4(d) are differential images where the derivative dz/dx is shown. They represent the surface as it appears when illuminated from the left. These images allow us to see more clearly the structure and Si clusters both inside and outside the crater. Amazingly, the lower left-hand corner is filled up much more rapidly than the upper right-hand corner. We also find that the $M2$ position of the upper right-hand corner remains unfilled until the very last moment [Fig. 4(d)]. When we reverse the direction of current, a preferential filling of the crater at the

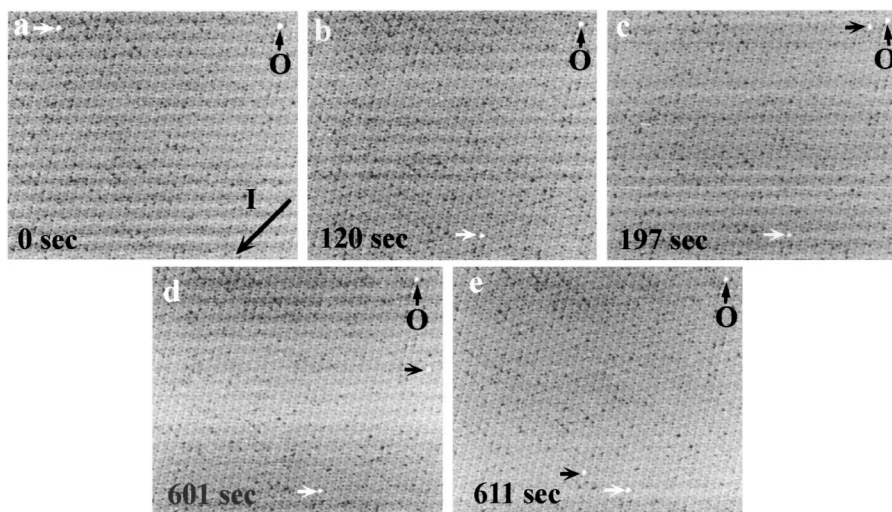


FIG. 2. The directed long hops of Si magic clusters on Si(111)-(7 × 7). These five images are chosen from our continuous-time scan of 9.2 s time interval each, taken at the sample bias of -2 V and at 450 °C. The image size is 800 Å × 670 Å. The current direction is indicated at the lower right-hand corner in (a), which is in the ascending step (step-up) direction of the substrate.

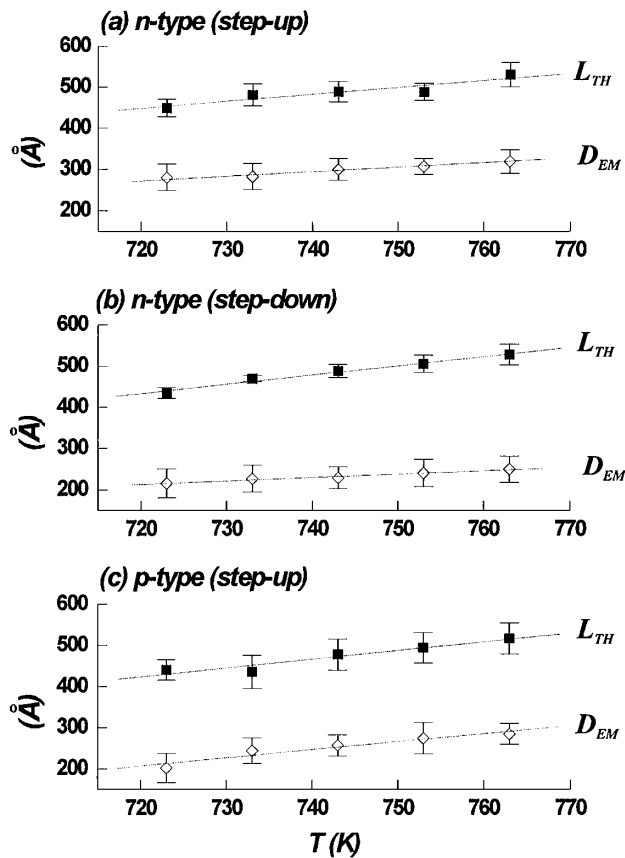


FIG. 3. Mean displacement length (D_{EM}) due to electromigration and mean thermal migration length (L_{TH}) obtained at different temperatures and for two different samples. The error bar is determined from the standard deviation of the related length. For both *n*-type and *p*-type samples, the bias in diffusion is along the direction of current. Each data point is calculated from displacements of ~ 100 (~ 60) long hops for the *n*-type (*p*-type) sample. The resistivity is $0.05 \Omega \text{ cm}$ and $0.01 \Omega \text{ cm}$ for the *n*-type and *p*-type samples, respectively. The step-up (step-down) direction indicates that the heating current is along the ascending (descending) step direction of the substrate.

upper right-hand corner is seen. Evidently, this anisotropy is caused by the electric field (current) across the sample. There is a concentration of Si magic clusters moving on the surface at temperature above 400°C [10]. Their migration is mainly along the direction of the heating current. Some of them may fall into the craters and migrate to the edge near the cathode side, resulting in preferential filling of that edge. A similar behavior was observed earlier [15], but no preferential filling in relation to the current direction was recognized.

In addition, we find that 2D Si islands tend to decay from the edge near the cathode side. Si islands can be prepared either by Si deposition at elevated temperatures [16] or by applying an electric pulse to the STM tip at elevated temperatures [14]. Figure 5 shows the decay process of a Si island by detachment of Si magic clusters. Clearly, the lower left-hand edge decays more rapidly than the upper right-hand edge. It is evident that the electric field not

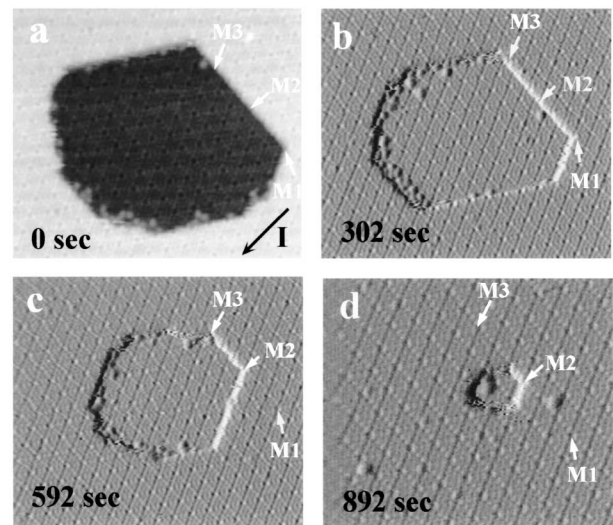


FIG. 4. Preferential accumulation of Si magic clusters and preferential filling of the Si crater at the lower left-hand corner. These images are taken at the sample bias of -2 V and at 480°C . Sites $M1$, $M2$, and $M3$ can serve as markers. The image size is $350 \text{ \AA} \times 300 \text{ \AA}$ for (a) to (c) and $300 \text{ \AA} \times 270 \text{ \AA}$ for (d). The current direction is the same as that indicated in Fig. 2.

only causes the directed migration of Si magic clusters, it also changes the rate of detachment of magic clusters from island edges. The electric field may also affect the incorporation or attachment of magic clusters to the step edge, resulting in the preferential filling of the crater seen in Fig. 4.

The driving force for electromigration is generally believed to consist of two parts: (1) direct force due to interaction between the diffusion species and the electric field,

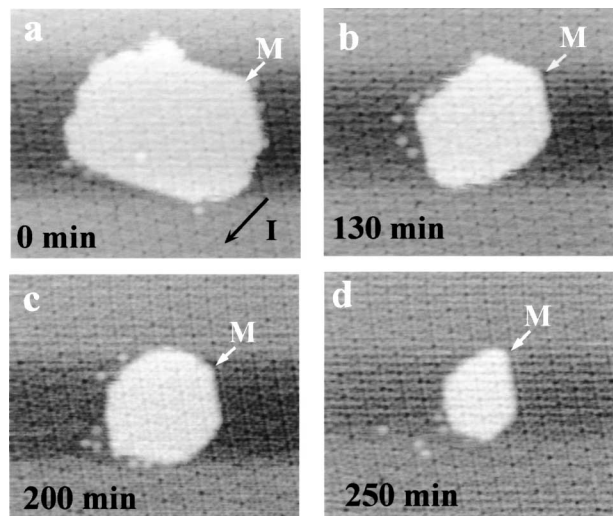


FIG. 5. Preferential dissociation of Si clusters from the lower left-hand edge of the island. Site M can serve as a marker. The image size is $450 \text{ \AA} \times 380 \text{ \AA}$. These images are taken at the sample bias of -2 V and at 450°C . The current direction is the same as that indicates in Fig. 2.

(2) carrier wind force due to momentum transfer in the scattering of the diffusion species by moving electrons or holes. The wind force can be ruled out because Si magic clusters show the same average net displacement in the direction of the heating current on both n -type and p -type samples. Also, the temperatures in our experiments are too low for the Si samples to have enough carrier density [17] to produce an appreciable wind force. As to the direct field force, Kandel and Kaxiras have proposed that the external electric field distorts the potential profile and thus induces a bias for diffusion on Si(111) surfaces [18]. The average fields in our samples (on the order of 1–10 V/cm, or 10^{-7} – 10^{-8} V/Å) appear to be much too low to produce such a strong diffusion bias seen in our system. A similar anisotropic diffusion of atoms on metal surfaces has been directly seen with field ion microscopy when an electric field gradient of the order of 0.1 V/Å^2 is applied [19,20]. Again, this field gradient is many orders of magnitude larger than what can exist in our samples. This raises the fundamental question about what is the nature of the driving force in electromigration of Si magic clusters.

Using STM potentiometry, Briner *et al.* have observed that scattering at surface defects can give rise to a potential discontinuity [21,22]. Similarly, the adsorption of a Si magic cluster may modify the local surface potential, such that the local field around the cluster is significantly larger than the average field. In addition, the diffusion barrier during the long hop may be very small, resulting in a strong bias in diffusion. The strong local field at island edges and at crater edges may also explain the anisotropy in attachment and detachment of magic clusters shown in Figs. 4 and 5. Since we have identified the diffusion species and studied the electromigration quantitatively on a well characterized Si(111)-(7 × 7) surface, thus Si(111)-(7 × 7) can be used as a model system for further theoretical study of the nature of the driving force in electromigration, and attachment and detachment of magic clusters at step edges under direct current heating. We believe an improved microscopic understanding of these processes is of great significance to semiconductor technologies as well as of fundamental importance to surface and materials sciences.

We acknowledge helpful discussions and comments of the manuscript by C.-S. Chang and W.-C. Wei. This work is supported by National Science Council (Contract

No. NSC88-2119-M-001-003) and Academia Sinica of R.O.C.

-
- [1] H. B. Huntington, in *Diffusion in Solids: Recent Development*, edited by A. S. Norwick and J. J. Burton (Academic Press, New York, 1975), pp. 303–352.
 - [2] P. S. Ho and T. Kwok, *Rep. Prog. Phys.* **52**, 301 (1989).
 - [3] B. H. Jo and R. W. Vook, *Appl. Surf. Sci.* **89**, 237 (1995).
 - [4] A. V. Latyshev, A. B. Krasilnikov, A. L. Aseev, and S. I. Stenin, *JETP Lett.* **48**, 526 (1988).
 - [5] A. V. Latyshev, A. L. Aseev, A. B. Krasilnikov, and S. I. Stenin, *Surf. Sci.* **213**, 157 (1989).
 - [6] S. Stoyanov, *Jpn. J. Appl. Phys.* **30**, 1 (1991).
 - [7] Y.-N. Yang, E. S. Fu, and E. D. William, *Surf. Sci.* **356**, 101 (1996).
 - [8] A. H. Verbruggen, *IBM J. Res. Dev.* **32**, 93 (1988).
 - [9] I.-S. Hwang, R.-L. Lo, and T. T. Tsong, *Surf. Sci.* **367**, L47 (1996).
 - [10] I.-S. Hwang, M.-S. Ho, and T. T. Tsong, *Phys. Rev. Lett.* **83**, 120 (1999).
 - [11] The probability that a different cluster that jumps into the image is estimated to be smaller than 0.0023 at 450 °C. In addition, no bias in the jump direction would be observed if we did not measure the long hops of the same cluster (see Fig. 3).
 - [12] W. D. Luedtke and U. Landman, *Phys. Rev. Lett.* **82**, 3835 (1999).
 - [13] S. Yu. Krylov, *Phys. Rev. Lett.* **83**, 4602 (1999).
 - [14] A. Ichimiya, Y. Tanaka, and K. Ishiyama, *Phys. Rev. Lett.* **76**, 4721 (1996).
 - [15] I.-S. Hwang, R.-L. Lo, and T. T. Tsong, *J. Vac. Sci. Technol. A* **16**, 2632 (1998).
 - [16] B. Voigtländer and T. Weber, *Phys. Rev. Lett.* **77**, 3861 (1996).
 - [17] S. M. Sze, *Physics of Semiconductor Devices* (John Wiley & Sons, New York, 1981), p. 19.
 - [18] D. Kandel and E. Kaxiras, *Phys. Rev. Lett.* **76**, 1114 (1996).
 - [19] T. T. Tsong and R. J. Walko, *Phys. Status Solidi A* **12**, 111 (1972).
 - [20] T. T. Tsong and G. L. Kellogg, *Phys. Rev. B* **12**, 1343 (1975).
 - [21] R. G. Briner, R. M. Feenstra, T. P. Chin, and J. M. Woodall, *Phys. Rev. B* **54**, R5283 (1996).
 - [22] B. G. Briner, R. M. Feenstra, T. P. Chin, and J. M. Woodall, *Semicond. Sci. Technol.* **11**, 1575 (1996).